Linear Stability Analysis Of Self-adaptive Bogie And Solution To Carbody Instability

Qibin Wang[1*], Jingying Ren[1], and Mingwei Piao[2]

[1] College of Locomotive and Rolling Stock Engineering, Dalian Jiaotong University, Dalian, 116028, China
[2] Mechanical Engineering School, Dalian Jiaotong University, Dalian, 116028, China
[*] Corresponding author. E-mail: q_b_wang@163.com

Received: Oct. 08, 2023; Accepted: Nov. 29, 2023

High-speed rail stocks need to seek a more suitable system design method for optimizing the design configuration in terms of system integrity as a typical research case of nonlinear systems. The self-adaptive improvement design based on ICE3 series bogie transforms the complex primary hunting phenomenon into simple carbody instability problem by means of big data mining such as orthogonal decomposition or modal design, and makes the minimum allowable equivalent conicity λ_{emin} reduced to (0.03 - 0.05). The linear stability analysis shows that the carbody instability problem of the self-adaptive improved design is caused by the complex interface singularity of the anti-rolling torsion bar, which can be effectively improved by the semi-active inter-vehicles damping technique. Due to the strong robustness of the self-adaptive improvement design, it can be realized to cross the railway dedicated lines with different speed grades, and then conditionally improve the self-cleaning ability of detrimental wear.

Keywords: Self-adaptive Bogie; carbody instability motion; linear stability analysis; complex interface singularity; semi-active damping technique

http://dx.doi.org/10.6180/jase.202410_27(10).0006

1. Introduction

Improving the operating speed, ride comfort and component reliability of high-speed rail stocks (HSRS) is a significant challenge in the development of high-speed rail (HSR) technology while ensuring safety. The bogie and its suspension are pivotal components that impact the dynamic stability of HSRS [1]. Due to the potential for significant safety risks caused by the stochastic failure [2], semi-active control techniques have been considered instead of fully-active control, e.g., semi-active control for anti-hunting or secondary lateral damper [3, 4]. For higher speed operation of Italian Pendolino tilting trains on mountainous routes, Bruni [5, 6] suggested removing compound bolster and introduced fully-active control of the secondary suspension technology for smarter and more accurate control of train dynamics. However, considering the high cost and technology constraints, Isacchi et al. [7] proposed the implementation of an energy-free passive anti-hunting damper to enhance the stability of HSRS by trading off the two contradictory technical specifications of tangent line operation and curve negotiation.

However, unlike launch or road vehicles [8], large-scale non-smooth systems such as HSRS have complex constraint singularity challenges. As a result, HSRS dynamics cannot be improved solely through component design, but must also be optimized from the perspective of system integrity. It is crucial to consider the effect of altering suspension parameters on full-vehicle performance. To this purpose, the suspension parameters of the full-vehicle were analyzed and their impact on the stability performance of the full-vehicle was explained by full-vehicle root-trajectory method [9].

Based on the above research methods and ideas, and considering the special characteristics of Chinese HSR practice, this study proposes that the design of HSRS systems needs to return to a rational boundary condition, i.e. the minimum allowable equivalent conicity λ_{emin} is decreased to (0.03 - 0.05), and the assumption of small creep without spin is held only under this boundary condition when the actual equivalent conicity $\lambda_e < 0.10$, so as to realize the stabilization of hunting motion, and thus to decrease the dynamic effects of the wheel-rail contact. This boundary condition can be determined by referring to the relevant domestic and international experiences [10, 11].

Aiming at the primary hunting design defects of ICE3 series bogies on the German ICE (Inter-City Express) rails and the unreasonable wheel-rail matching influence [12], i.e. $\lambda_e \geq 0.10$, the following research results have been achieved in this study: 1) Self-adaptive improvement design has been formulated by utilizing big data mining techniques such as modal design of nonlinear systems or proper orthogonal decomposition [13];) Rigid-flex coupling simulation technology has been utilized to improve the flexible body to MBS (Multi-Body System) interface transacting strategy with finite element model correction technology based on the load type processing of the component interface, and the inherent rigid-flex coupling relationship of HSRS system has been reasonably constructed [14].

Compared to existing methods such as rail grinding, wheel profile replacement, brake grinding on wheel tread, and wheelset re-profiling under floor, the contribution of this study is to optimize the configuration of system parameters by linear analysis method, attempting to make HSRS strong-robust at the system design level. Moreover, the carbody instability at low equivalent conicity is solved without affecting the stability performance of the bogie. In this way, vehicles can operate on railway dedicated lines with different speed levels to achieve self-cleaning of detrimental wear.

Based on previous work, the self-adaptive high-speed bogie is taken as the research object in this paper, which firstly introduces the relevant theories of the analysis graph of full-vehicle stability properties and variation patterns. Then this method is used to carry out sensitivity analysis on the parameters of self-adaptive bogie in order to clarify the carbody instability problem to be solved. Finally, the pre-study analysis is conducted to determine the improvement direction for controlling the carbody instability by semi-active inter-vehicle damping technology with the theory related to the skyhook strategy.

2. Nonlinear systems modal design for HSRS

Unlike general road vehicles, there are complex constraint singularities in rail vehicle systems, so undifferentiated MBS processing cannot be achieved for rail and road vehicles. Moreover, there is a possibility of ill-condition in the Jacobian matrix obtained from the linearization of the rail vehicle system. For this reason, the improved generalized augmentation method proposed by Negrut rapidly identifies the direction of least resistance perturbation direction by a clever combination between generalized independent variables and virtual augmentation variables.

For high-speed rail vehicles, MBS simulation models contain (non-) holonomic constraints, i.e. $C = C_1 \cup C_2$ and index-3 differential algebraic equations (DAEs) as follows:

$$M\ddot{q} + C_q^T \gamma = Q \tag{1}$$

in which, M is the mass matrix; Q is the system external force including the non-conservative forces; γ is the undetermined factor, which is combined with the transposition of Eq. (2) to constitute the system internal force.

$$C_q \equiv: \frac{\partial C}{\partial q} \tag{2}$$

However, the generalized space variable q must satisfy the following constraints: 1) holonomic constraints $C_1 = 0, \dot{C}_1 = 0, \ddot{C}_1 = 0$; 2) non-holonomic constraints $C_2 = 0, \dot{C}_2 = 0$. Therefore, q can be further divided into two subsets: i.e. $q = y \bigcup x$.

Generally, the space state reduction method needs to meet preconditions for non-singularity, i.e. $\det(C_x) \neq 0$. However, some software attempts to avoid complex constraint singularities through model simplification and wheel rail table lookup, thereby forming a multidisciplinary collaborative simulation design based on equal step integration algorithm. For this reason, True objects to the use of equal step integration algorithms [15], due to the difficulty in controlling the singularity of complex constraints. Although the calculation is complicated and inefficient, Negrut's variable-step integration algorithm with three stages of prediction-correction-evaluation has been sufficiently validated in solving the engineering problems such as complex constrained internal forces, details seen in references [16–18]. Esp., as long as the correctness of the initial conditions is fully guaranteed, accurate analysis results of complex constrained internal forces can be obtained.

Consequently, considering the algorithm's issues with complexity and inefficiency, assuming that it is to be optimized for the design of large and complex nonlinear systems, a big data mining method is required to determine the direction for improvement.

The analysis graph of full-vehicle stability properties and variation patterns is a useful optimization tool for the modal design of nonlinear HSRS systems. The dialectical relationships of wheel-rail contact exhibit near-linear or nonlinear characteristics based on the mechanical properties of lateral non-conservative systems. Hence, the proper orthogonal decomposition technique should be employed to optimize the parameters of the high-speed bogie to decouple non-linear vibration interactions for attaining the desired steady state.

In each steady state with constant speed, it is assumed that the quasi-equilibrium state can be described by the Eq. (3) for the rail vehicle MBS system.

$$F(y, \dot{y}, t) = 0 \tag{3}$$

in which, y represents all steady state variables.

At the working point, $y = y^k$ and $\dot{y} = \dot{y}^k$, the first order difference formula of Eq. (4) is given as follows:

$$\left[\left. \frac{\partial F}{\partial y} \right|_{y^k, \dot{y}^k} + \frac{1}{h\beta_0} \left. \frac{\partial F}{\partial \dot{y}} \right|_{y^k, \dot{y}^k} \right] \Delta y = -F(y, \dot{y}, t) \tag{4}$$

in the formula, β_0 is the scalar constant, which is related to the integrator order; Δy is the corrected difference direction; h is the integration step size; $-F$ is the residual part of Eq. (4), which represents the imbalance degree of the force system.

Assuming $\boldsymbol{u}$ and $\dot{q} = u$, and designating $\bar{q}, \bar{u}$ as the virtual augmentation variables, Eq. (1) will be reduced to first-index DAEs:

$$\left. \begin{array}{c} M\dot{u} + P\gamma = Q \\ B_1 u = \bar{u} \\ B_0 q = \bar{q} \end{array} \right\} \tag{5}$$

in which, $P = P(q) = (\partial C / \partial q)^T$ is a projective operator, which represents the partial differential transformation relation of (non-) holonomic constraints as shown in]Eq. (2); B_0 and B_1 are the Boolean matrices; the rest of the notation is consistent with Eq. (1).

The left matrix of Eq. (4) is the F Jacobian matrix on the required quasi-equilibrium state, i.e. the Jacobian matrix of first-index DAEs [1].

$$J(v, \lambda_e) = \begin{bmatrix} \frac{M}{h\beta_0} - C_u & M_q \dot{u} + C_{qq}^T \gamma - Q_q & C_q^T \\ E & -\frac{1}{h\beta_0} & 0 \\ 0 & C_q & 0 \end{bmatrix} \tag{6}$$

in the matrix, E is the unit matrix; u, q, qq are subscripts, i.e. the first or second order partial derivatives of (non-) holonomic constraints C to u or q.

Accordingly, the MBS eigenvalue solution $\text{Eig}(J(v, \lambda_e))$ can be acquired through the orthogonal decomposition. Subsequently, the analysis graph of full-vehicle stability properties and variation patterns can serve as a closed-loop system root trajectory for reflecting the stability properties of the full-vehicle as well as the visual analysis means of the pattern changes due to alterations in system parameters.

Compared with the conventional root locus graph, it has three major characteristics: 1) avoiding the limitation of quasi-static perturbation simulation of open-loop system, and instead focuses on closed-loop poles; 2) examining the crucial damping property of some kinematic modes of the dynamical system, which are prone to self-excited vibration; 3) the convected motion relationship, i.e. a linear correlation between relevant modes that arises due to the singularity of the complex interfaces in a generalized space.

In summary, there are two linearization methods for general nonlinear systems: one yields analytical results when the Jacobian matrix satisfies the positive semi-definite condition, producing mode orthogonality and modal shape (anti-) symmetry; the other assumes complex constraint singularities causing the Jacobian matrix to be ill-conditioned, which then results in energy exchange between relevant modes through convected motion relationships. At this point, orthogonality and symmetry are no longer satisfied.

3. Carbody instability and parameter sensitivity analysis

3.1. Self-adaptive bogie and its technical features

Compared with the original design of the German ICE3 series bogie, as shown in Fig. 1, the parameter configurations were optimized in the self-adaptive improvement design. Its key technical characteristics are summarized below:

1) A reasonable matching relationship is established between the anti-hunting damper dynamical features and wheelset positioning constraint stiffness, which results in the conversion of carbody yaw mode from over-damped to small-damped, and enhances the yaw phase margin of both front and rear bogies.

2) A beneficial "anti-phase effect" is robustly formed between the bogie hunting motion and the associated motor hanger swing motion. When $\lambda_e < 0.20$, the motors and their hangers swing with opposite yaw to prevent the rapid attenuation of the relative bogie yaw phase margin; whilst $\lambda_e \geq 0.20$, the modal vibration of motor hanger tends to be unstable;

3) There is carbody instability problem in the range of speed (160-200) km/h when $\lambda_e < 0.10$. It should be noted that the motion is independent of the phase margin of either front or rear bogie yaw.

To ensure its suitability for a range of railway lines and

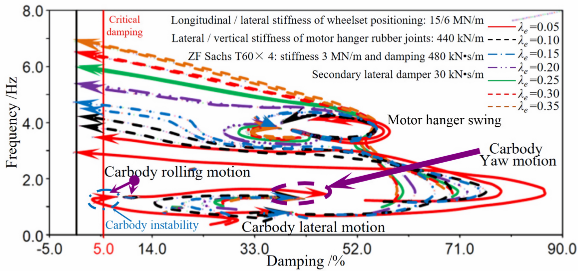

(a) Analysis graph of full-vehicle stability properties and variation patterns

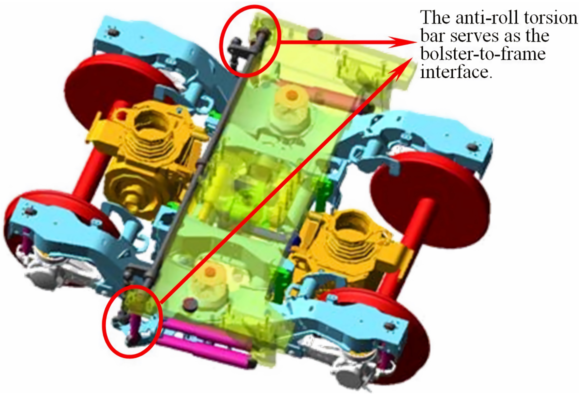

(b) Schematic diagram of bogie model

Fig. 1. Self-adaptive high-speed bogie and its technical features

to enhance adaptability, the self-adaptive improvement design still needs to solve the carbody instability problem and eliminate the carbody shaking and related negative impacts whilst minimizing technical costs.

The nonlinear system dynamics simulation model of the full-vehicle is linearized, and the results of the minimum damping ratio of the system modes of the full vehicle are simulated and analyzed by the system modal calculations as shown in Table 1 for the carbody self-excited speed of 200 km/h.

Table 1. Lateral kinematic modes of the in-service vehicle (v = 200 km/h, λ_e = 0.05)

Mode	Frequency/Hz	Damping/%
Carbody lateral motion	0.75	35.51
Carbody yaw	1.34	15.96
Carbody rolling	1.25	5.61
Front bogie hunting	1.50	69.99
Rear bogie hunting	0.79	77.90

It can be seen from Table 1 that the frequencies of the carbody yaw and rolling mode are similar, but the proportional damping of the rolling mode is smaller and close to the critical damping of 5%. Combined with Fig. 1, the carbody instability motion is caused by the self-excited vibration of the carbody rolling mode under a certain condition of v = (160 - 200) km/h and $\lambda_e \leq 0.10$, which is not attributable to the external excitation but belong to the lateral instability problem. Therefore, the solution to the carbody instability problem can be defined as follows: under the boundary condition of $\lambda_{emin} \leq$ (0.03 - 0.05), the system parameters should be reasonably designed to enable self-adaptive bogie to remove the above-mentioned motion without the primary hunting feature. The primary hunting feature refers to the formation of a convected motion relationship between the rear bogie hunting motion and carbody rolling mode under the over-damped of the carbody yaw.

Based on numerous theoretical and experimental studies on the parameters that impact HSRS operation stability, in order to identify the root causes of the carbody instability phenomenon, the sensitivity analyses are carried out mainly on the suspension parameters, so as to formulate optimization countermeasures.

For the ICE3 series bogies, the primary or secondary suspensions that affect the lateral instability are: the positioning stiffness of the rotating arm axlebox, secondary lateral dampers, secondary air springs, anti-hunting dampers, and anti-roll torsion bars, respectively. A parameter sensitivity analysis of the above suspensions is carried out to determine the causes of the carbody instability motion and to formulate feasible technical countermeasures.

3.2. Sensitivity analysis of bogie suspension parameters

For primary suspension, a sensitivity analysis is conducted on the positioning stiffness of the rotating arm axlebox. The MARK 4 passenger trains of the British Railways face serious wheel wear problems, the incorporation of hydraulic joint for axlebox rotating arm in the bogie primary suspension is suggested with higher technical risks [19].

As shown in Fig. 2, when λ_e = 0.05 and the longitudinal wheelset positioning stiffness (15 - 25) MN/m, the analysis graph presents parameter insensitive changes. If the longitudinal wheelset positioning stiffness continues to increase, the carbody instability problem is somewhat mitigated, but the primary hunting phenomenon reappears. In other words, once the longitudinal wheelset positioning stiffness is greater than 26 MN/m, it cannot form a reasonable matching relationship with the dynamic characteristics of the anti-hunting damper. Also, considering the high technical risk of the hydraulic joint of the rotating arm, it is not feasible to improve the carbody instability by adjusting the wheelset positioning stiffness.

For the secondary suspension, the sensitivity analysis

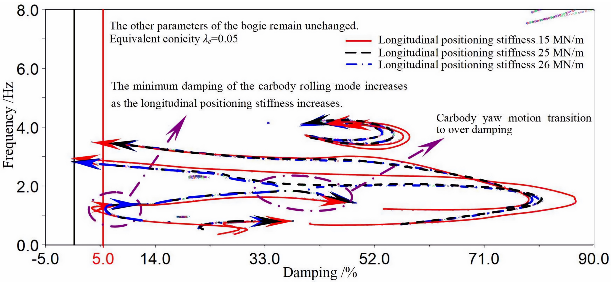

Fig. 2. Sensitivity analysis of bogie primary suspension parameters affecting lateral dynamic performance

is first performed for the anti-hunting damper parameters. Considering that the new anti-hunting damper adopts the vibration reduction technique of high-frequency resistance action introduced, its damping is parametrically analyzed.

With other suspension parameters unchanged, as shown in Fig. 3a, by decreasing the anti-hunting damper linear damping calibration, the analysis graph shows that once the linear damping calibration value is reduced to 415 kN·s/m and below, the carbody yaw mode is transformed into over-damped characteristic, and the yaw phase margin of front and rear bogies becomes significantly attenuated. And the self-excited vibration state is still present in the carbody rolling mode. Considering the current level of manufacturing process, higher damping cases for the anti-hunting damper are not considered. Therefore, the anti-hunting damper is not sensitive to the carbody instability problem under the low conicity studied in this paper.

As for the secondary lateral damper in which the stiffness is very small in general, thus its linear calibrated damping value is analyzed for sensitivity. As shown in Fig. 3b, the analysis graph shows that the carbody instability phenomenon still exists no matter increasing or decreasing the damping of the secondary lateral damper. Considering the dissipation term of the non-conservative system, decreasing the damping of the secondary lateral damper will exacerbate the degree of carbody shaking. When the damping of the secondary lateral damper is increased to 35 kN·s/m, the carbody yaw mode appears over-damped characteristic, which forces the phase margin of the rear bogie yaw evidently insufficient. The analysis of its stiffness parameters also shows a similar phenomenon. Although the secondary lateral damper can dissipate some kinetic energy of carbody shaking, the solution is not feasible due to the reappearance of the primary hunting feature and the improper configuration of the system dynamics parameters.

For the secondary suspension with adjustable parameters, the sensitivity analysis of the air spring parameters

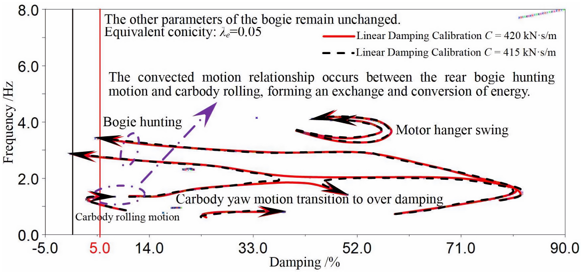

(a) Anti-hunting damper damping

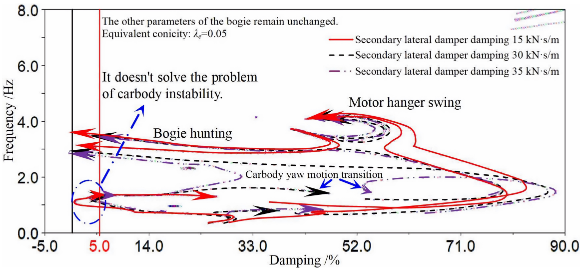

(b) Secondary lateral damper damping

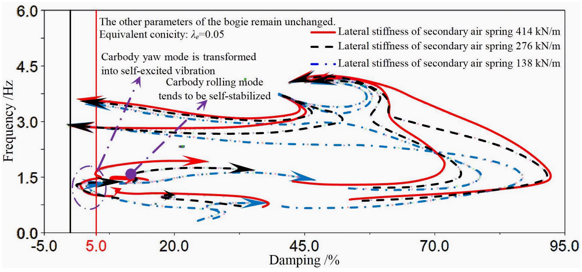

(c) Secondary air spring lateral stiffness

Fig. 3. Sensitivity analyses of bogie secondary suspension parameters affecting dynamic performance

is carried out, which analyzes the air spring connection on both sides, the diameter size of the orifices, the volume of the auxiliary air compartment, and the lateral stiffness, respectively. The results show that, except for the lateral stiffness of the air springs, which affects the lateral modes of the carbody, as shown in Fig. 3c, the rest of the parameter configurations only affect the damping and frequency of the vertical modes of the carbody (not shown in the text).

Under the original configuration parameter of 138 kN/m, the lateral stiffness of air spring is increased to twice and four times respectively. The analysis graph that the phase margin of bogie yaw is significantly reduced by the increase of the lateral stiffness of the air springs. Both the modal characteristics of the carbody yaw and rolling change as a result, with the damping of carbody yaw decreasing and the damping of rolling modes increasing. Although the carbody rolling mode tends to be self-stabilized with the increase of the air spring lateral stiffness, the carbody yaw mode is transformed into self-excited vibration.

Therefore, it is not feasible to solve the carbody instability problem by changing the air spring parameters.

Based on the above scheme attempts and the sensitivity analysis of each suspension parameter of the bogie, it is necessary to clarify the reasons for the formation of the carbody instability motion problem at low conicity investigated in this paper, and to reformulate a feasible scheme.

4. Complex interface singularity for anti-rolling torsion bars

The anti-rolling torsion bar, as one of the important interfaces between the carbody and the bogie, as shown in Fig. 1b, is the medium for energy exchange and singularity change between the carbody and the bogie modes, and contributes to the carbody stiffness in a nonlinear way.

The design principle of anti-rolling torsion bar device is such that there is a perturbation direction of minimum resistance at both ends of the torsion bar, regardless of its floating or fixed simple support. According to the principle of elastic potential energy conversion, the contribution to the carbody rolling stiffness mainly depends on the radial stiffness of the rubber joints between the pull rods on both sides and the bolster of bogie [20]. Therefore, it can be seen that if the safety and stability margin is sufficient or good lateral dynamics of HSRS, the torsion bar is not enough to affect system stability properties.

However, if the high-speed shaking phenomenon occurs at low conicity, the anti-rolling torsion bar will make a nonlinear contribution to the stiffness of the carbody rolling direction, and the frequency of the carbody rolling is ca. 1.2 Hz. During the speed increase test of the Beijing-Shanghai HSR, it was observed that the train experienced high-speed shaking with main frequency of 2.3 Hz when its running speed was increased to 300 km/h, instead of the self-excited vibration of the carbody rolling modes. Therefore, the anti-rolling torsion bar will not provide stiffness contribution to the rolling direction of the carbody at this time. Moreover, the negative effects of wheel creep are intensified by the primary hunting phenomenon or carbody instability due to the inactive anti-roll torsion bar.

Thus, it can be inferred that the improper use of anti-rolling torsion bar device may result in the singularity change of complex constraints, i.e. the force transfer path changes. As shown in Fig. 4, assuming that the anti-rolling torsion bar is inactive, the minimum damping of the carbody rolling mode will be higher than the critical damping, and there is no problem of carbody instability. It is evident that the carbody instability existed for the self-adaptive improvement design is link to the inappropriate use of the anti-rolling torsion bar device.

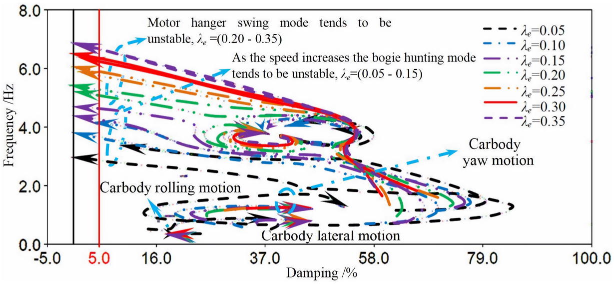

Fig. 4. Analysis graph of full-vehicle stability properties and variation patterns for the anti-rolling torsion bar device inactive

However, it should be noted that it is impossible to remove the anti-rolling torsion bar device due to the frequent operation of HSRS on elevated lines with crosswinds, side winds, and wake disturbances. The carbody instability problem in self-adaptive improvement is still not negligible. Therefore, the self-adaptive improvement should deal with carbody instability problem at lower economic and technical cost, and eliminate the carbody shaking phenomenon and its negative effects.

5. Pre-study analysis of inter-vehicles damping based on the skyhook strategy

The carbody instability problem caused by the self-excited rolling vibration is becoming more significant and adversely affecting the quality of train operation. To improve the comfort and safety of HSRS, vibration damping measures such as addition of vibration dampers at the carbody end or improving the original carbody end connection equipment can be used to attenuate the relative motion between vehicles.

To enhance the efficacy of the inter-vehicle damping device against carbody instability motion, it is necessary to carry out the pre-research and analysis of inter-vehicles damping based on the single-vehicle skyhook strategy as shown in Fig. 5. According to the Kelvin parallel model, it is calculated that when the lateral torsional stiffness is 74.629 MN·m/deg, its operational frequency is approximately the frequency of the carbody yaw mode as shown in Table 1, at ca. 1.2 Hz.

When the equivalent conicity $\lambda_e = 0.05$, vertical torsional damping of 200 kN·m·s/deg and lateral torsional damping of 600 kN·m·s/deg are applied, as shown in Fig. 6, it is found that the carbody rolling mode is annihilated (i.e. the modal damping is greater than 100%), and the minimum damping of the carbody yaw mode is higher than the critical damping by 5%, while the bogie yaw phase margin is still sufficient.

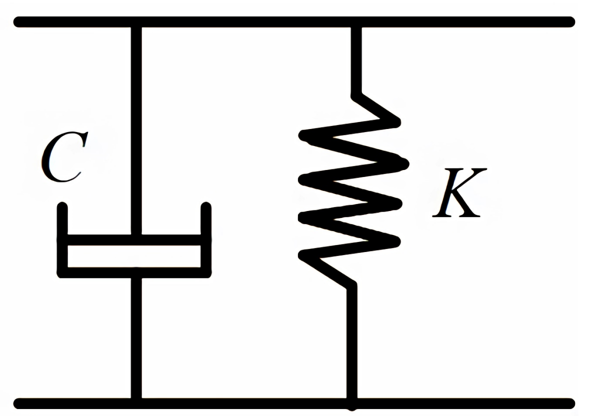

(a) Kelvin model

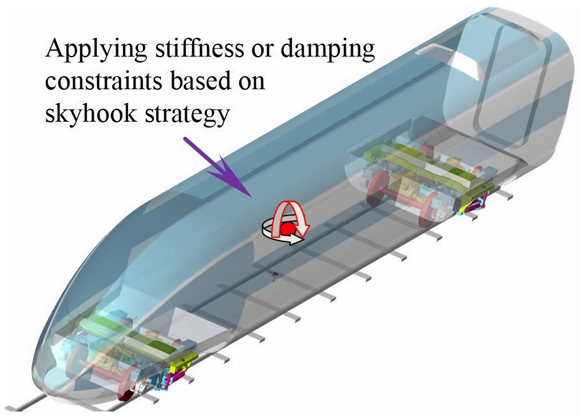

(b) Pre-study based on single vehicle

Fig. 5. Pre-study analysis of inter-vehicles vibration damping based on a single vehicle

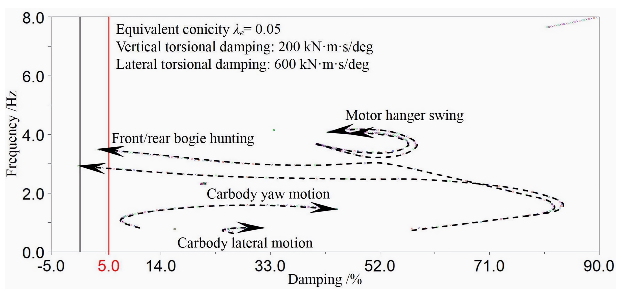

Fig. 6. Analysis graph with torsional damping applied at $\lambda_e = 0.05$

However, by continuing to decrease the equivalent conicity, the low-conicity carbody instability reappeared. As a result, the lateral torsional stiffness of 74.629 MN·m/deg is applied according to the Kelvin model. When equivalent conicity $\lambda_e = 0.05$, as shown in Fig. 7a, the minimum damping of both lateral and vertical modes of carbody is higher than the critical damping by 5%. The carbody rolling mode tends to be self-stabilized without

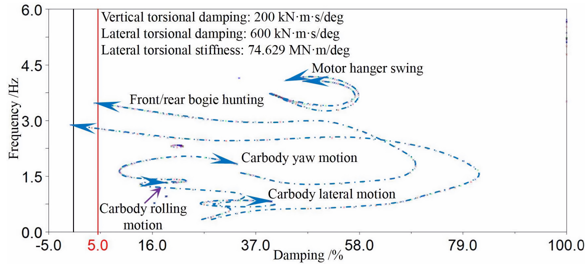

(a) $\lambda_e = 0.05$

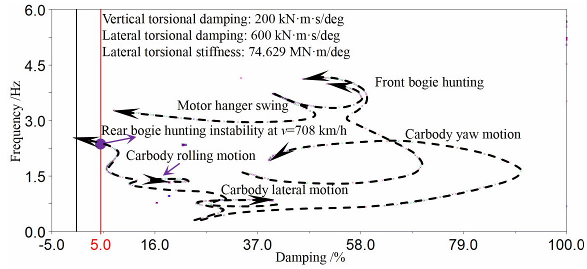

(b) $\lambda_e = 0.04$

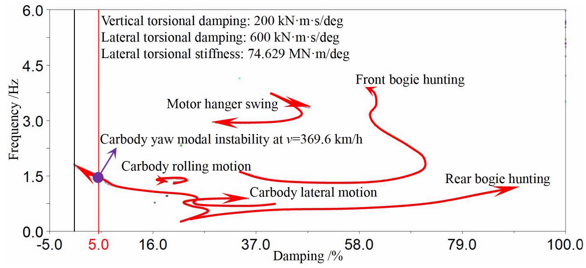

(c) $\lambda_e = 0.03$

Fig. 7. Analysis graph with torsional damping and stiffness applied at different equivalent conicity

coupling between the carbody and the bogie. As for the equivalent conicity reduced to 0.04, as shown in Fig. 7b, the stability property of the full-vehicle has changed significantly, i.e. the carbody yaw mode is transformed from a small-damped to an over-damped state, but there is no convected motion relationship between the bogie hunting mode and the carbody rolling mode which tends to be self-stabilized. Accordingly, the maximum critical speed reaches 708 km/h. Nonetheless, when $\lambda_e = 0.03$, the first mode of instability is the carbody yaw, in which its linear critical speed reaches 369.6 km/h. Additionally, the minimum damping of the carbody rolling mode is higher than the critical damping of 5% with tendency to be self-stabilizing state. The carbody instability problem has been solved by the control law of the semi-active damping device, i.e. the semi-active device is activated when the vehicle speed is (160 - 200) km/h and the comfort index exceeds 2.5.

For carbody instability motion of self-adaptive high-speed bogie, the carbody up-swing vibration can be attenuated by semi-active inter-vehicles damping technology with reference to the carbody-end damping technology of Japanese Shinkansen HSRS. In order to attenuate the up-swing vibration of the in-service carbody, the carbody-end damper consists of two dampers with double pivoting arms and a connecting rod. The front and rear carbody end walls support the dampers, which attach to the connecting rod through double swivel arms. When there is a change in the distance between the vehicles or the relative swing angle, the two dampers absorb the kinetic energy of the carbody up-swing motion by the double swivel arms, and the dampers are quickly recovered using springs simultaneously. Specifically, dynamic simulation verification has been conducted on the effectiveness of semi-active inter-vehicles damping technology based on three-vehicle trainset [21], confirming the improvement effect of inter-vehicles damping devices on ride comfort and the good of self-adaptive bogie.

6. Conclusion

(1) The primary hunting design defect of the ICE3 series bogies exacerbates the central hollow tread wear. Self-adaptive improvements are more favorable to commercial use than wheel-rail relationship improvements. However, adjusting the bogie parameter configurations alone cannot solve the problem of carbody instability at low conicity and may cause sudden parameter changes to shock the behavior of the in-service vehicle system.

(2) The linear stability analysis with the removal of the anti-rolling torsion bar device provides insight into the solution to this problem: i.e. the imposition of the torsional damping and stiffness in the direction of the carbody rolling and yaw can improve the carbody instability motion. Compared with rail grinding or wheelset re-profiling under floor, inter-vehicles damping technology can solve the carbody instability problem with cost-effective.

(3) The analysis graph of full-vehicle stability properties and variation patterns refers to the stability properties reflected in the root trajectory map of the closed-loop system, and big data mining means such as orthogonal decomposition or modal correction are used to clarify the right direction of self-adaptive improvement, so that the nominal model of the bogie can be returned to the canonical perturbation problem in the sense of asymptotic stability, and satisfy two major requirements, i.e. smoothness and ergodicity.

References

[1] L. Cui, G. Li, C. Song, A. Wang, X. Li, and R. Luo, (2021) *"Study on Optimization of Suspension Parameters of High-speed EMU Trains"* **Journal of the China Railway Society *43***(4): 42–50. DOI: 10.3969/j.issn.1001-8360.2021.04.006.

[2] Y. Zeng, D. Song, W. Zhang, Z. Hu, and Z. Chang, (2021) *"Stochastic failure process of railway vehicle dampers and the effects on suspension and vehicle dynamics"* **Vehicle System Dynamics *59***(5): 703–718. DOI: 10.1080/00423114.2019.1711136.

[3] X. Wang, B. Liu, E. Di Gialleonardo, I. Kovacic, and S. Bruni, (2022) *"Application of semi-active yaw dampers for the improvement of the stability of high-speed rail vehicles: mathematical models and numerical simulation"* **Vehicle System Dynamics *60***(8): 2608–2635. DOI: 10.1080/00423114.2021.1912366.

[4] Z. Gao, B. Tian, D. Wu, and Y. Chang, (2021) *"Study on semi-active control of running stability in the high-speed train under unsteady aerodynamic loads and track excitation"* **Vehicle System Dynamics *59***(1): 101–114. DOI: 10.1080/00423114.2019.1662924.

[5] E. Di Gialleonardo, A. Facchinetti, and S. Bruni, (2023) *"Control of an integrated lateral and roll suspension for a high-speed railway vehicle"* **Vehicle System Dynamics *61***(2): 472–498. DOI: 10.1080/00423114.2022.2049319.

[6] S. Alfi, S. Bruni, R. Goodall, and C. Ward, (2023) *"Secondary yaw control to improve curving vs. stability trade-off for a railway vehicle"* **Vehicle System Dynamics *61***(5): 1367–1386. DOI: 10.1080/00423114.2022.2094277.

[7] G. Isacchi, F. Ripamonti, and M. Corsi, (2023) *"Innovative passive yaw damper to increase the stability and curve-taking performance of high-speed railway vehicles"* **Vehicle System Dynamics *61***(9): 2273–2291. DOI: 10.1080/00423114.2022.2105242.

[8] J. T. Allison and D. R. Herber, (2014) *"Special section on multidisciplinary design optimization: multidisciplinary design optimization of dynamic engineering systems"* **AIAA journal *52***(4): 691–710. DOI: 10.2514/1.J052182.

[9] H. Shi, J. Zeng, and S. Qu, (2023) *"Linear stability analysis of a high-speed rail vehicle concerning suspension parameters variation and active control"* **Vehicle System Dynamics *61***(11): 2976–2998. DOI: 10.1080/00423114.2022.2147086.

[10] M. Zacher, D. Nicklisch, G. Grabner, O. Polach, and B. Eickhoff, (2015) *"A multi-national survey of the contact geometry between wheels and rails"* **Proceedings of the Institution of Mechanical Engineers, Part F: Journal of Rail and Rapid Transit** ***229***(6): 691–709. DOI: 10.1177/0954409714568171.

[11] Y. Muhamedsalih, G. Tucker, and J. Stow, (2023) *"Optimisation of wheelset maintenance by using a reduced flange wear wheel profile"* **Proceedings of the Institution of Mechanical Engineers, Part F: Journal of Rail and Rapid Transit** ***237***(2): 253–265. DOI: 10.1177/09544097221105959.

[12] M. Piao, J. Yang, D. Liu, J. Fang, and D. Tian, (2016) *"Design defaults of German ICE3 serial bogies and technical solutions"* **Computer Integrated Manufacturing Systems** ***22***(7): 1654–1669. DOI: 10.13196/j.cims.2016.07.005.

[13] T. Li, M. Piao, J. Fan, Z. Fang, S. Jin, and G. Li, (2022) *"Dynamical design of self-adaptive high-speed bogies based on full-vehicle stability properties and variation patterns"* **Computer Integrated Manufacturing Systems** ***28***(2): 385–408. DOI: 10.13196/j.cims.2022.02.006.

[14] T. Li, W. Du, M. Piao, Y. Guo, S. Jin, C. Nie, J. Fang, Y. Cheng, and J. Fan, (2021) *"Dynamical effect investigations of component's internal interface by using techniques of rigid-flex coupling simulation"* **Shock and Vibration** ***2021***: 1–13. DOI: 10.1155/2021/6509950.

[15] H. True, A. P. Engsig-Karup, and D. Bigoni, (2014) *"On the numerical and computational aspects of non-smoothnesses that occur in railway vehicle dynamics"* **Mathematics and Computers in Simulation** ***95***: 78–97. DOI: 10.1016/j.matcom.2012.09.016.

[16] D. Negrut and J. L. Ortiz, (2006) *"A practical approach for the linearization of the constrained multibody dynamics equations"* **Journal of Computational and Nonlinear Dynamics** ***1***(3): 230–239. DOI: 10.1115/1.2198876.

[17] E. Haug, D. Negrut, and M. Lancu, (1997) *"A state-space-based implicit integration algorithm for differential-algebraic equations of multibody dynamics"* **Journal of Structural Mechanics** ***25***(3): 311–334. DOI: 10.1080/08905459708905292.

[18] D. Dopico, F. González, J. Cuadrado, and J. Kövecses, (2014) *"Determination of holonomic and nonholonomic constraint reactions in an index-3 augmented Lagrangian formulation with velocity and acceleration projections"* **Journal of Computational and Nonlinear Dynamics** ***9***(4): 041006. DOI: 10.1115/1.4027671.

[19] C. Qu, Y. Li, J. Jiang, G. Tucker, S. A. Neild, M. Smith, A. Gleeson, S. Odetunde, and Y. Muhamedsalih, (2023) *"Reducing wheel–rail surface damage by incorporating hydraulic damping in the Bogie primary suspension"* **Vehicle System Dynamics** ***61***(8): 1916–1936. DOI: 10.1080/00423114.2022.2092012.

[20] M. Piao, C. Guo, W. Du, G. Li, and J. Fan, (2021) *"Influences of anti-rolling torsion-bar fixed/floated simple supports to formations of detrimental worn treads"* **Journal of Dalian Jiaotong University** ***42***(5): 59–65. DOI: 10.13291/j.cnki.djdxac.2021.05.011.

[21] Q. Wang, S. Piao, M. Piao, P. Dang, Q. Li, and J. Ren, (2023) *"A Dynamic Design Methodology for Large-Scale Complex Nonlinear Systems Based on Orthogonal Decomposition Technique"* **Shock and Vibration** ***2023***: DOI: 10.1155/2023/7152223.